

# Revealing Secrets From Pre-trained Models

Mujahid Al Rafi, Yuan Feng, Hyeran Jeon  
University of California, Merced  
{mrafi, yfeng44, hjeon7}@ucmerced.edu

**Abstract**—With the growing burden of training deep learning models with large data sets, transfer-learning has been widely adopted in many emerging deep learning algorithms. Transformer models such as BERT are the main player in natural language processing and use transfer-learning as a de facto standard training method. A few big data companies release pre-trained models that are trained with a few popular datasets with which end users and researchers fine-tune the model with their own datasets. Transfer-learning significantly reduces the time and effort of training models. However, it comes at the cost of security concerns. In this paper, we show a new observation that pre-trained models and fine-tuned models have significantly high similarities in weight values. Also, we demonstrate that there exist vendor-specific computing patterns even for the same models. With these new findings, we propose a new model extraction attack that reveals the model architecture and the pre-trained model used by the black-box victim model with vendor-specific computing patterns and then estimates the entire model weights based on the weight value similarities between the fine-tuned model and pre-trained model. We also show that the weight similarity can be leveraged for increasing the model extraction feasibility through a novel weight extraction pruning.

## I. INTRODUCTION

Machine learning has been rapidly adopted to virtually almost all the computing fields from image recognition to natural language processing. The accuracy and performance of machine learning models determine the solution providers' market revenue. To acquire startups that provide outstanding machine learning solutions, big tech companies spend billions of dollars recently. Therefore, the machine learning model implementation details are one of the top priority secrets that the solution providers need to protect. However, recent a few studies demonstrated that it is feasible to steal model topology, hyperparameters, and training dataset [1], [2], [3]. These attack models, namely *model extraction attack*, *hyperparameter stealing attack*, and *membership inference attack* leverage side channels through performance counters, cache access timings, and bus probing. Most of the existing attack models targeted models used for image processing such as convolutional neural network (CNN). Though revealing model architectures is possible, it is known to be very challenging to reveal actual weight values due to the abundant size. Some recent studies revealed one- to eight-bit weight values from ResNet model with an extended RowHammer attack method [4]. To recover 80 ~ 90% accurate weight values, they had to run at least 4000 hammer-leak rounds.

In this paper, we show an easier way to reveal almost accurate weight values as well as model structure by exploiting a recent model training trend. To save model training time and also

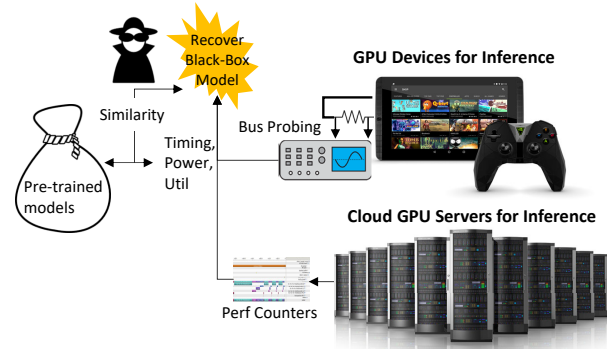


Fig. 1: Proposed Attack Model

develop more accurate models with larger dataset, transfer-learning has been widely adopted. Transformer model and its variants such as BERT [5] and GPT [6], [7] follow transfer-learning. A few big data companies release general-purpose models that are pre-trained with large un-labeled datasets and individual developers and other companies develop their own model by fine-tuning the pre-trained model with their own datasets. Due to the obvious cost and performance benefit of transfer-learning, it is very rare to develop these models from scratch. For example, the pre-trained BERT-base and GPT-2 models released on the Huggingface model repository have been downloaded more than 10 million times and 20 million times, respectively [8], [9]. However, we observed that the pre-trained models are double-edged sword that not only provides model development efficiency but also exposes model secrets unintentionally. From our observation, many fine-tuned models show very high similarities in weight values with the baseline pre-trained models. Once an attacker grabs the information about the baseline pre-trained model with various adversarial attack methods [1], [2], [3], the black-box fine-tuned model's weight values can be easily estimated without thousands to millions of memory probing.

Regarding the adversarial attacks, unlike existing studies assumed, we observed that system statistics do not show unique pattern for individual models. Even for the models that use the same architecture and are trained with the same dataset for the same task (e.g., BERT-large for question-answering task trained with SQuAD dataset), the system statistics show notable variances if the models are released by different vendors and use different frameworks. We observed that individual vendors tend to use unique sets of GPU kernels mainly due to different framework usage and optimization preferences, which lead to diverse system statistics. Therefore, we found that the existing

model extraction attack methods show good extraction accuracy only when the victim model uses exactly the same GPU kernels that the adversary developed the attack model with. On the other hand, we found that such vendor/framework signatures are a good source of information about the pre-trained model that the black-box model is developed with. As a pre-trained model and its fine-tuned model have very similar weight values, once the baseline pre-trained model is identified, almost similar weights can be revealed in a whole model level.

In this paper, we present a new model extraction attack that leverages the vendor/framework signatures and weight value similarity to extract model architecture as well as weight values. We also propose weight extraction pruning that significantly reduces the memory probing and hammering scopes in finding the exact weight values by leveraging the uncovered pre-trained model’s weights and the typical value distances between pre-trained models and their fine-tuned models. In summary, we show an easier and more accurate model extraction attack for transfer-learning based models. We show examples and evaluations with mostly BERT models but the ideas can be extended to any models that use transfer-learning, as we show a CNN example in Section VI. Figure 1 illustrates the proposed attack model where an adversary uses not only system statistics but also patterns found from pre-trained models for recovering a black-box model.

Our contributions are like below:

- 1) We show novel observations that can be leveraged for developing a more accurate model extraction attack for transfer-learning based models: 1) high value similarity between a pre-trained model and its fine-tuned model and 2) vendor/framework signature in architecture statistics
- 2) We develop a new model extraction attack that recovers not only the victim model architecture but also the entire (almost similar) weight values by exploiting the aforementioned two observations. With our proposed weight extraction pruning, the actual weight values can be more easily recovered.
- 3) To our best knowledge, this is the first study that extracts architecture of Transformer models. Our observation shows that the architectural uniqueness of Transformer models eases the extraction and hence an adversary does not need to check multiple side-channels; only the GPU-side function execution time monitoring is sufficient.

## II. TRANSFORMER-BASED MODELS

Though transfer-learning can be technically used by any machine learning algorithms, one of the most popular models that use transfer-learning as default training method is Transformer model. Transformer models have proved their effectiveness in various domains including natural language processing (NLP) and computer vision [10]. Especially in NLP, Transformer is efficient to be adapted to several diverse tasks such as question answering, sentiment analysis, named entity recognition, etc with a task-specific last layer attached to the baseline pre-trained model architecture. In spite of large model size, Transformer models gain popularity due to its

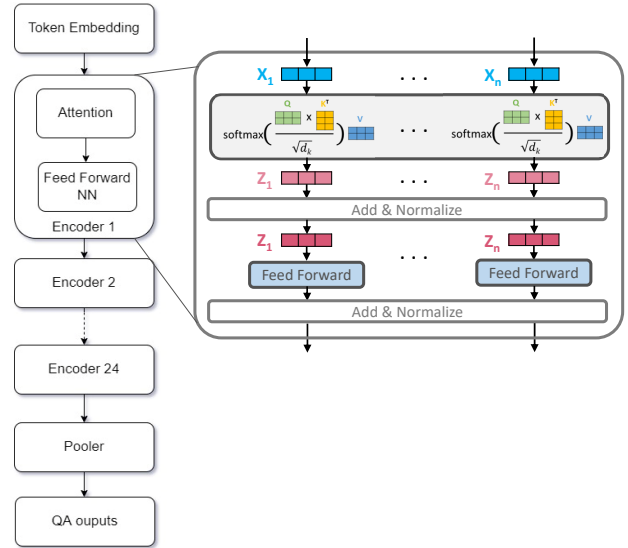


Fig. 2: BERT-large Architecture

parallel architecture. Unlike earlier NLP solutions that relied on recurrent and convolution computations, Transformer models focus on attention computations. By extracting relations across input tokens, Transformer locates the most influential parts of the input that determine the output prediction. A Transformer model runs multiple rounds of attention computations where each attention layer checks relations across all tokens of the given input in parallel.

Transformer models can consist of one (or both) of two key modules: *encoder* and *decoder*. Each *encoder* is further comprised of two layers: self-attention and feed-forward, as illustrated in Figure 2. The unique algorithmic strength of Transformer models is sourced from the self-attention layer. In a self-attention layer, properly embedded input tokens are multiplied with three weight matrixes, namely Key ( $W_k$ ), Query ( $W_q$ ), and Value ( $W_v$ ) and generate K, Q, and V vectors. These three vectors for each token are used for understanding the importance of the token in the input context. Then *attention scores* are calculated via a multiplication of Q vector and K vector followed by a normalization ( $\alpha$ ) and a softmax operation. Then, the attention score is applied to V vector to calculate a weighted Value,  $V'$ .  $V'$ 's are accumulated to a Z vector and passed to a feed-forward layer, and then to the next encoder. After going through cascaded encoder layer computations, a task-specific layer computes a classification result to generate a prediction output. The overall computation is depicted in Equation 1.

$$Z = \text{Softmax}\left(\frac{Q(i) \cdot K(i)^T}{\alpha}\right) \cdot V(i) \quad (1)$$

Decoders share a similar architecture with encoders, except for one key difference. While an encoder processes the whole input hidden states at once, a decoder only processes one hidden state in a single forward computation. This leads to a slight difference to self-attention layer where a decoder uses masked self-attention such that future tokens are excluded from the computation.

While Transformer models are introduced to solve problems in machine translation domain, several Transformer variant models are proposed to the other domains with keeping similar model architecture. The variants can be summarized into two groups: 1) discriminative models, such as BERT [5], RoBERTa [11], ALBERT [12], which only contain the encoders and 2) generative models, such as GPT-2 [6] and GPT-3 [7] which contain either decoders only or both encoders and decoders. Though any number of encoders and decoders can be used for building a model, there are several well-evaluated reference models such as BERT-base, BERT-large, GPT-2 medium and large, and GPT-3. Out of them, we use BERT and its variant models as the main attack targets in this paper. The main differences between BERT-base and BERT-large models are the number and size of encoders where BERT-base uses 12 encoders with 12 attention heads each while BERT-large includes 24 encoders with 16 attention heads each. The internal layers of each encoder are the same, as described above. The BERT-large architecture is illustrated in Figure 2.

### III. MOTIVATIONS

#### A. Weight Value Similarity

To understand the relation between pre-trained models and their fine-tuned models, we compared weight values of four BERT implementations, as can be seen in Figure 3. We tested the pre-trained and fine-tuned BERT (RoBERTa) Large models released by three vendors, Huggingface [13], Meta [14], and NVIDIA [15], [16]. We compared the absolute value of individual weights of the Value weight matrix ( $W_v$ ) used by the self-attention computation in each encoder layer. Each square in the Figure 3 is a value similarity heat map for  $1024 \times 1024$   $W_v$  per encoder. As illustrated on the right-hand side color map, black-colored entries mean the weight value in the same location of each weight matrix of the pre-trained model and the fine-tuned model have high similarity (almost no difference), while the white-colored entries indicate that the value distance between the pre-trained and fine-tuned weights are almost 0.2. Surprisingly, the models of Huggingface and Meta show very minimal value disparity ( $< 0.002$ ) for all encoder layers. The NVIDIA-released fine-tuned model shows higher differences but it is also not very significant, where the averaged difference is around 0.025. When we fine-tuned the released pre-trained model with the vendor provided fine-tuning script (without changing anything), the weight similarity became higher, like Huggingface and Meta, as can be seen in Figure 3(d). It seems that NVIDIA might have applied some optimizations over the fine-tuning script for the released fine-tuned models, but again the weight difference was insignificant. Though we show only  $W_v$  value comparisons results due to the limited space, weights for Query and Key also had similar patterns.

One might think that the value similarity is sourced from small weight values. However, the weight value ranges of the tested BERT-large models are at least 1.74 up to over 26.3, as can be seen in Figure 5. To investigate if such high value similarity is found only between a pre-trained model and its own fine-tuned model, we did another comparison between different

vendors-released models, as can be seen in Figure 4. With the same color scale, we observed notably higher differences in this case, where the averaged value gap is around  $0.075 \sim 0.1$ . We suspect that fine-tuning hyper-parameter values play some role for this similarity. According to our observations, the fine-tuning scripts provided by all the examined vendors use up to three epochs with small learning rates, which is around  $3e-05$ . Therefore, fine-tuned models might have very subtle differences from the pre-trained models. To understand if the similarity is caused purely by the fine-tuning parameters, we also measured the weight value changes while running longer epochs. Figure 6 shows the average weight value changes of  $W_v$  of encoder 22 and task-specific output layer (question-answer task in this example) of an NVIDIA BERT-large PyTorch model collected while fine-tuning a vendor-released pre-trained model for 30 epochs. The weights of  $W_v$  have average of 0.001 difference at epoch 3 compared to the pre-trained model, which is also shown in Figure 3(d). Until epoch 9, weight difference increases up to 0.0015 and then drops linearly to below 0.0002 at epoch 30. In the meantime, the output layer's weights are saturated exponentially as plotted in the second graph in Figure 6, which means that the fine-tuning converges well. These results show that fine-tuning may achieve better accuracy with more epochs but the weight values do not significantly change even with longer epochs. The reasons can be twofold: 1) pre-trained models are already highly trained with large dataset and 2) fine-tuning is more like an adaptation process for a general-purpose pre-trained model to be used for a specific task. Therefore, the most important step of fine-tuning is not changing the weights in vast majority of the model architecture but attaching a task-specific last layer to a pre-trained model and tuning the weights slightly to fit well for the fine-tuned task.

In the perspective of performance and prediction accuracy, weight value similarity between pre-trained model and its fine-tuned model may not raise any concerns. However, in security aspect, this fact can be leveraged to extract weight values from a black-box fine-tuned model. Once the model architecture and the vendor is recovered, weight values can be estimated to be within  $< 0.002$  value range from the vendor's publicly accessible pre-trained model. Note that anybody can access pre-trained models as pre-trained models are considered as public resources for transfer-learning models.

#### B. Vendor & Framework Signatures

To extract victim model architecture, we investigated the common characteristics of various Transformer models such as BERT and RoBERTa. Interestingly, we observed quite diverse statistics from the models released by different vendors even when the models use the same architecture. Figure 7 shows time-series execution times of kernels launched by individual models on the same GPU. Each dot indicates the execution time of a kernel and the same-colored dots are the multiple invocations of the same kernel. Each graph plots the statistics of a BERT-large model that is fine-tuned and released by the specified vendor for question-answering task and uses the stated framework. Meta's is RoBERTa-large that basically uses the same model

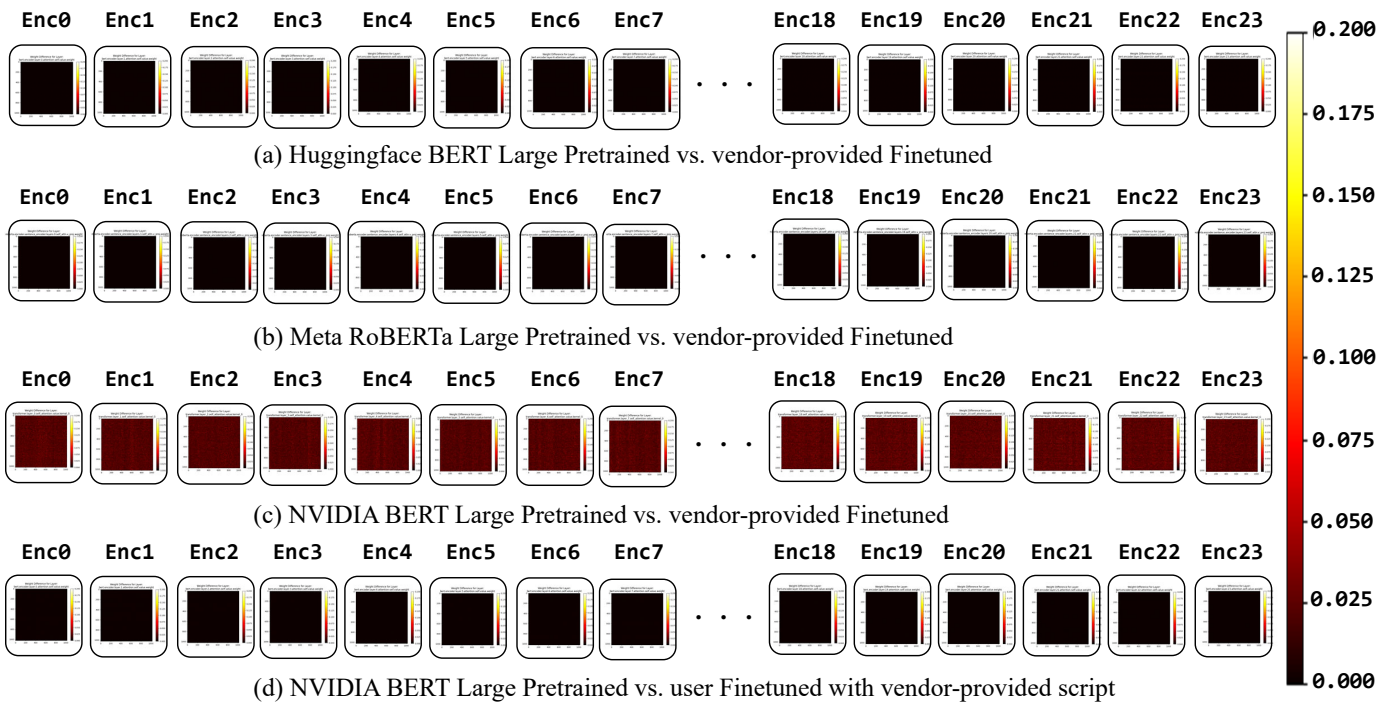


Fig. 3: Per-Encoder Weight ( $W_v$ ) Value Similarities between Pre-trained model vs. Fine-tuned model: weight difference color map on right (black : higher similarity, white : lower similarity)

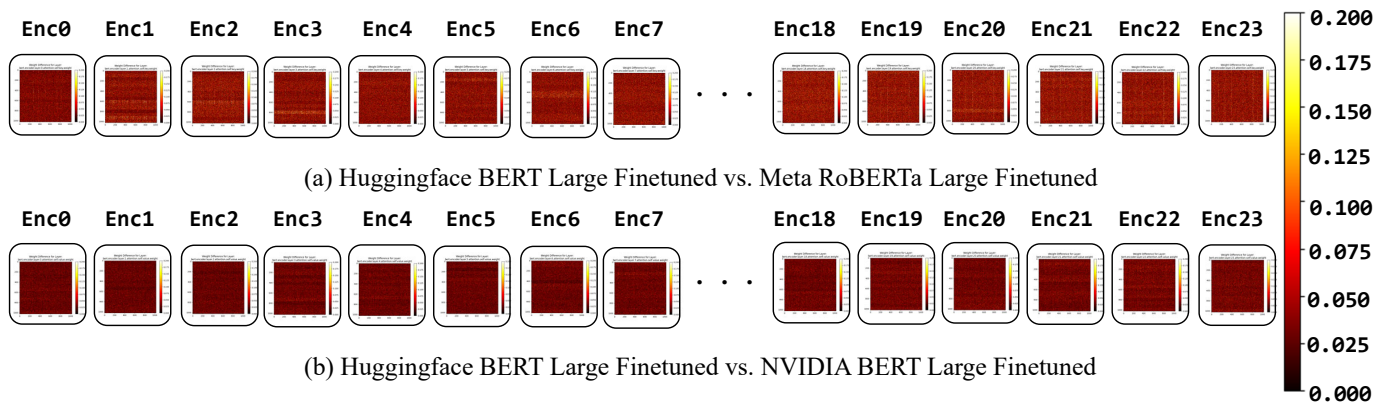


Fig. 4: Per-Encoder Weight ( $W_v$ ) Value Similarities between Different Vendor Models

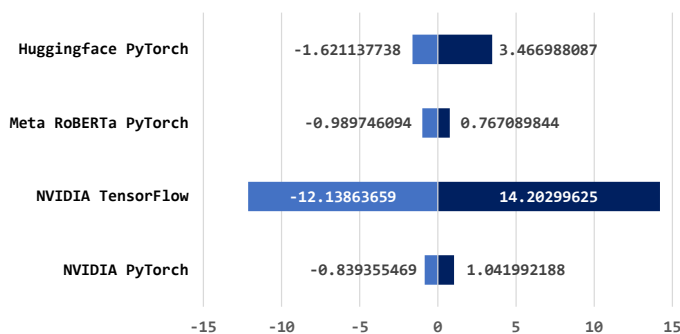


Fig. 5: Weight Value Range of BERT-large Models

architecture with BERT-large while using different datasets for pre-training. All models are tested with the same input.

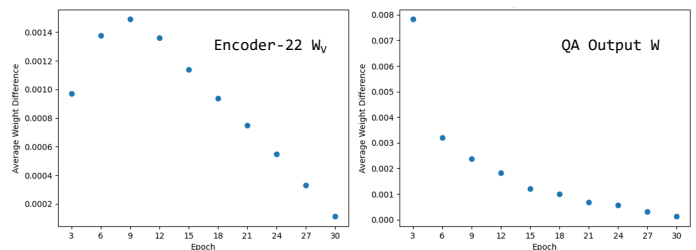


Fig. 6: Avg. Weight Changes during 30-Epoch Fine-tuning

As can be seen, there are not common patterns found across them. However, for each vendor's models that use the same framework, the statistics show high consistency even when they are fine-tuned for different tasks. Figure 8 shows the results of the same test for NVIDIA PyTorch BERT-large models that are

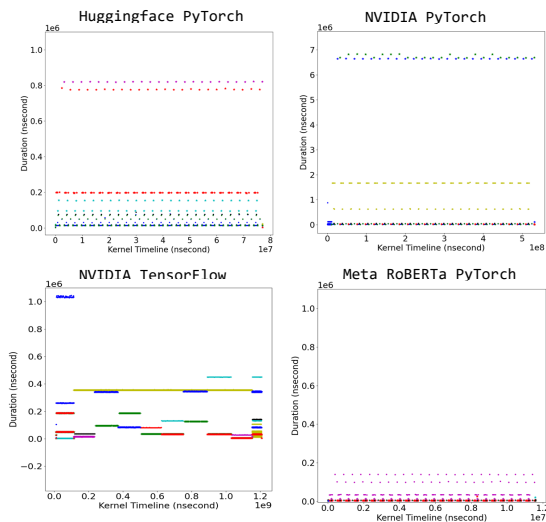


Fig. 7: Diversity in Time-series Kernel Execution Times for BERT-large Models Released by Different Vendors

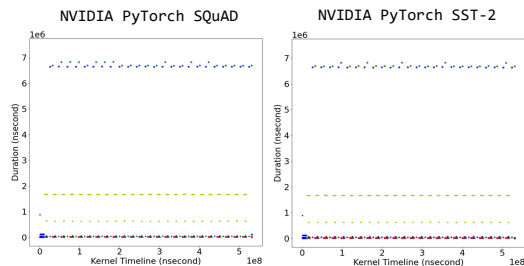


Fig. 8: Consistency in Time-series Kernel Execution Times for BERT-large Models Trained for Different Tasks Released by One Vendor

finetuned for (left) question answering and (right) sentiment analysis. Though there are some diversity in GPU kernel usage, the vast majority of kernels used by both models are identical and the statistics show almost indistinguishable patterns. We observed such vendor-unique statistics for all tested models. We call this as *Vendor Signature*.

The vendor signature is mainly sourced from individual vendors’ preference for algorithms and frameworks, which leads to different GPU kernel selections. Figure 9 shows the list of kernels executed by BERT-large models of different vendors and frameworks. Though the same model architecture was executed, only one kernel (`splitKreduce_Kernel`) was commonly used by all the listed four models. From the kernel usages, we found that the most notable differences appear between different frameworks. TensorFlow models run  $5 \times \sim 8 \times$  more kernel executions and use almost  $40 \times$  more unique kernels than PyTorch models. Also, TensorFlow models tend to use their GPU backends (e.g., `Mul_GPU_DT_FLOAT_DT_Float`, `convert`, `fusion`, etc.), while PyTorch models use more GPU library functions (e.g., `volta_sgemm`). Vendor-specific kernel preferences are also observed. Though different frameworks were used, NVIDIA models are commonly optimized to leverage their Tensor Core by running functions using half-precision (fp16) data types. On the other hand, Meta models tend to

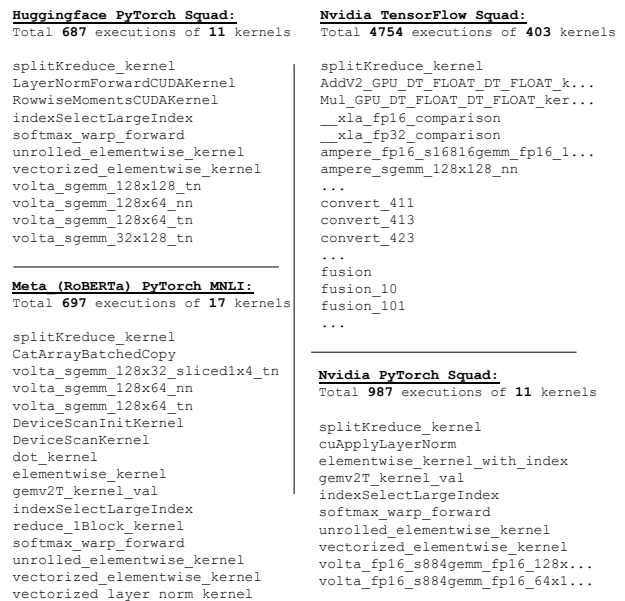


Fig. 9: Kernels Executed by BERT-large Models

run many short kernels such as reduction operations (e.g., `reduce_1Block_kernel`, `DeviceScanKernel`, etc.) and hence the statistics have crowded kernel executions on the bottom of the graph.

The vendor signatures do not only lead to kernel execution time pattern disparity. All the related architecture hints that are commonly leveraged by many model extraction attacks become different and hence the attack success rate can be significantly reduced. As most of architecture-hint-based model extraction attacks have targeted CNN models, we tested a state-of-the-art CNN model extraction attack [1], which is designed for PyTorch models (though the authors did not discuss framework impacts), with statistics of various models that use different frameworks and released by different vendors. Figure 10 shows layer detection results when the attack model is tested with ResNet-101 models in PyTorch and TensorFlow versions. The red-colored layers are mis-predictions. There is notably higher error rate when using different framework even when the models use the same CNN architecture. Table I shows the layer prediction errors when testing with various models. LER means how many layers are incorrectly predicted per layer [1]. Thus, LER over 1 means that the prediction results can’t be considered as having meaningful results. From this result, we also observed that even when using the same framework, if the model is released by different vendors (see the result of NVIDIA PyTorch in the table) and hence uses different GPU kernels, the prediction accuracy drops significantly.

To our best knowledge, there has not been a study that considers the impact of vendor and framework for model extraction attacks. As it is hard for an adversary to know what kind of software stack the victim black-box model uses, the attacks have higher noise than the earlier studies reported. In our study, we show how the vendor signatures can be incorporated to improve attack success rate by identifying the

TABLE I: Impact of Framework and Vendor Optimizations for CNN Layer Detection Accuracy

Models	Error Rate (LER)	Kernel Seq. Length	# of Unique Kernels
DeepSniffer Original Results [1]	0.091	222	16
DeepSniffer Pytorch Model [17]	0.567	256	16
Nvidia PyTorch Model [18]	2.628	1235	38
Google Tensorflow Model [19]	6.274	3399	50
Amazon Mxnet Model [20]	6.768	2652	59

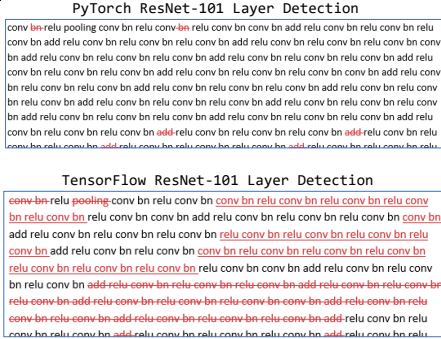


Fig. 10: Impact of Framework for CNN Model Extraction Attack Accuracy: layer detection errors are colored red

pre-trained model used by the black-box fine-tuned model. As noted earlier, once the baseline pre-trained model is located, the weights can be easily estimated for a whole model.

#### IV. THREAT MODEL

Unlike existing studies that either recover model architecture or weight values for mostly CNN-based solutions, we show that both model architecture and weights can be recovered for Transformer models. Due to the different information granularity, where architecture extraction requires individual kernel execution pattern whereas weight extraction needs bit-level information, we assume different scoped threat models for each target information.

**Adversary Identity:** Figure 1 illustrates the overall architecture of our threat model. We assume that an adversary is either an end-user that has a physical access to the device that the victim model is deployed or an admin of a cloud server where the victim model is running. The admin attacker may or may not have physical access to the server but he/she can at least run GPU performance/memory profiler that can measure various architectural characteristics. The adversary is assumed to have a large pool of pre-trained models that are at least publicly accessible. With the model pool, the adversary is assumed to have good knowledge about various vendor and framework signatures at least that can be observed from the target system that the victim model is deployed.

**Model Architecture Extraction:** Our architecture extraction model is a blackbox attack, where adversaries do not have any information about the model architecture. To identify the model architecture (the boundary, number, size, and algorithm of encoders that determine the victim model), the adversary measures GPU kernel execution time. If the adversary has a physical access to the target machine, he/she can use electromagnetic (EM) side-channel attack on interconnects between CPU and GPU [21]. If the adversary is an admin, GPU performance profiler provides sufficient information about

individual kernel execution times. These side-channels are accessible as many earlier studies assumed [1], [2], [3].

**Weight Extraction:** The proposed weight extraction is a graybox attack, where the adversary is aware of the victim model architecture through the above model architecture extraction method. We explore two methods to extract weights: selective weight checking and heuristic testing-based weight estimation. For the selective weight checking, the adversary can acquire weight file address range through EM side-channel attack or memory profiling and check the weight values through either row hammering or bus probing, like earlier studies assumed [1], [2], [3], [4], [22]. For the heuristic testing, the attacker estimates the weights through fine-tuning of a pre-trained model with datasets that are related to the victim model’s task. Thus, the only capability that the attacker additionally has is to run the victim model with various inputs and check the prediction outputs, which requires general user-level capability.

#### V. MODEL EXTRACTION

Inspired by the observations, we propose a new model extraction attack that exploits weight-value similarity and vendor & framework signatures. We use BERT models as the main attack targets in this paper, though the same methods can be used for any models that follow similar architectures.

##### A. Model Architecture Extraction

We examined various architecture hints such as DRAM reads and writes, cache misses and accesses, kernel execution time, the total number of kernels invoked during the inference, and so on for various fine-tuned models. We found that the time-series kernel execution time reveals sufficient model architecture information for the target BERT models. This is because BERT models use fairly regular architectures unlike other models such as CNNs. A CNN model uses different types of layers (though mostly convolution, pooling, and fully-connected) without strict ordering, and the individual layers use different weight size and number of neurons. Therefore, a combination of multiple arch hints is needed to identify layer boundaries and types of layers. However, Transformer models including BERT run identically-shaped encoders repeatedly and hence architecture hints also show repetitive patterns. Therefore, a group of repeated measurements can be considered as one encoder. The encoders of any BERT models use the same internal layers as described in Section III while the volume of computations may vary. Such encoder size can be also detected with kernel execution time because larger encoders consume longer execution time, which we will show the actual statistics soon. Therefore, we use a time-series kernel execution time as the only side channel for our attack model.

We assume that the kernel execution time is measured through EM side-channel attack on interconnects or a performance profiler, as assumed in the Threat model in Section IV. Note that kernel execution time is less vulnerable to noise because a probing frequency that is several hundred nano-second- to mili-second-scale is sufficient to detect individual

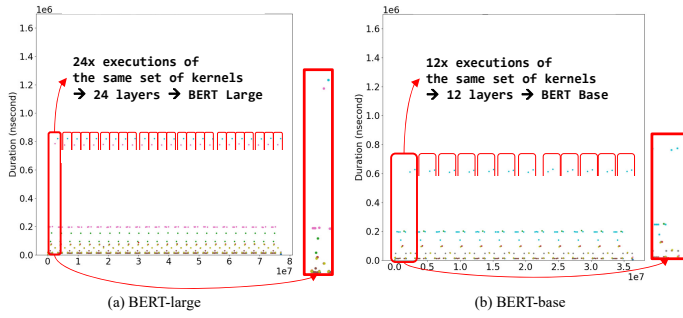


Fig. 11: Encoder Boundary Identification from Time-series Kernel Execution Times: Each dot reflects the execution time of one GPU kernel

kernels and kernel boundaries do not need intra-GPU chip probing; bus activities between CPU and GPU are sufficient. Our noise sensitivity study shows robust model architecture prediction accuracy with various noise levels. Details can be found in Section VI-B.

1) *Recovering Encoder Boundary & Count*: Figure 11 shows layer identification examples for BERT-base and BERT-large PyTorch models. In each kernel execution time graph, it is easy to observe that a unit of multiple kernels is repeatedly executed. The box on each graph is the unit of kernel group. The zoom-in version is next to each graph. By partitioning the graph vertically for each kernel-group unit, BERT-base has 12 repeated patterns and BERT-large has 24 of them, which are matching with the number of encoders of each model architecture. In other words, the unit of kernel group is corresponding to one encoder execution. Without identifying individual intra-encoder layers and dependencies across encoders, the boundary of encoders and the number of them can be easily recovered.

Encoder boundary identification of PyTorch models are straightforward. However, as can be seen in Figure 7, NVIDIA TensorFlow model’s statistics show notably different patterns. From digging into the script, we found that NVIDIA TensorFlow model by default uses XLA optimization [23]. After disabling the optimization, the TensorFlow model execution also showed clear encoder boundaries. Figure 12 shows three execution patterns of TensorFlow models. Left two graphs show NVIDIA TensorFlow models with and without XLA optimizations and the right-most graph is Huggingface TensorFlow model that does not use any optimization. It turns out XLA optimization runs compiler optimization operations in the middle of inference, as marked as XLA region. The executions for encoders are in the beginning and ending of the inference (outside the XLA regions). In both encoder regions, we were able to find 24 repetitive kernel group executions, as plotted in Figure 13. Huggingface model had a slight difference, where there is only one region that has 24 group executions followed by a long last layer execution. Therefore, Huggingface TensorFlow model architecture can be identified similar to PyTorch model detection method.

For the NVIDIA TensorFlow models, especially when XLA option is enabled, the vast majority of execution is spent

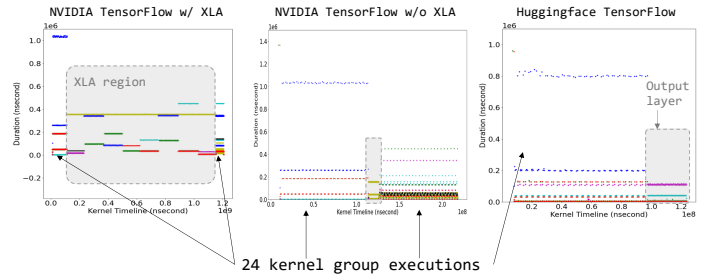


Fig. 12: TensorFlow Model Execution Patterns with/wo Optimizations

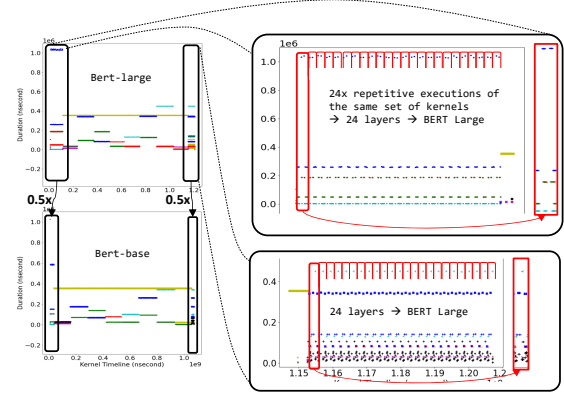


Fig. 13: Encoder Boundary Identification for TensorFlow Models with XLA

for XLA computations as shown in Figure 13. The length and statistics of XLA region are similar in different BERT architectures. Therefore, the statistics cannot be directly used for encoder detection. Instead, we propose to develop a model that identifies the encoder regions. Within the encoder regions (highlighted with black boxes in the beginning and ending of each model graphs), the encoder detection method used for PyTorch models can be reused. The red lines show clear encoder boundaries in the zoom-in graphs on the right side of the Figure 13. XLA is a TensorFlow-specific optimization. Similarly, there are other vendor-specific and framework-specific optimizations that add noise for model extraction. Therefore, one method can’t be used for all. However, as far as there is any consistency found from similar models, the attacker can always make an alternative solution, just like we did for XLA optimization cases; we were able to locate the encoder region because XLA-enabled BERT-large and BERT-base models show similar patterns.

2) *Recovering Encoder Size*: Though the number of encoders provide enough information to distinguish BERT architecture, we also observed that encoder size is detectable from the kernel execution time graph. Note that BERT-base has 12 encoders where each encoder contains 12 attention heads with weight dimensions as  $768 \times 768$ , while BERT-large has 24 encoders where each encoder includes 16 attention heads with weight dimensions as  $1024 \times 1024$ . Therefore, an encoder of a BERT-large model needs around 70% more computations than that of BERT-base model. In all tested models, we consistently observed that the longest kernel’s execution time of BERT-

large models is at least 20% longer than that of BERT-base models. For example, in Figure 11, a BERT-base model’s peak kernel execution time is around  $0.6 \times 1e6$  ns (= 0.6 ms) while the same vendor’s BERT-large model’s is around 0.8 ms. In Tensorflow models, the execution regions that have architecture hint have notable peak execution time differences as can be seen in Figure 13; BERT-base’s peak kernel execution time is around 0.43 ms while BERT-large’s is over 1 ms. With the profiled typical peak kernel execution time, it is possible to estimate the encoder size.

3) *Recovering Intra-Encoder Architecture*: Though the size and number of encoders vary, all BERT model variants use the same encoder architecture as described in Section III. Each encoder consists of a self-attention layer and a feed-forward layer. If intra-encoder layers and algorithms are the targets to leak (in case the victim model makes some optimizations on encoders), we observed that some post-processing on the kernel execution time statistics enables layer and algorithm detection.

Figure 14 shows example per-layer and algorithm execution times of BERT-large and BERT-base models. In both models, we were able to find that feed-forward layers take over  $2 \times$  longer execution times than attention layers. For each attention layer, the Key, Value, and Query vector calculations equally consume the most time. The attention score calculation is the second most time-consuming operation. Softmax and layer-norm operations are consistently very short. Therefore, from this layer- and algorithm-boundary analysis, adversary will be able to identify encoder architecture. For example, if there are more than three equal-length layers that consume the highest time within each attention layer, the adversary can catch that the victim model is using one more core vectors besides, Key, Value, and Query. Also, if per-layer execution time is less than typical duration, the adversary can suspect other optimizations such as head pruning. We discuss the pruned head prediction in Section V-B3.

This layer- and algorithm-boundary detection needs vendor signature detection apriori because each layer typically runs multiple kernels, and different vendors and frameworks use different kind of kernels, as discussed with Figure 9. We assume that the attacker already has vendor signature information through exhaustive evaluations.

4) *Automated Model Architecture Extraction*: To automate the attack process, there are two challenges: 1) the kernel group shape varies due to vendor signatures and 2) the kernel groups can be only distinguishable in the time domain, which means individual kernels’ execution times as well as invocation timing information are needed to distinguish kernel group repetitions. Therefore, the automation needs to be able to 1) detect kernel groups when the groups have different size and shape and 2) process a 2-dimensional information, where each dimension indicates the kernel invocation sequence and individual kernel execution time. We found that this problem can be reduced to a pattern recognition problem for 2-dimensional inputs, which is similar to image recognition. Each kernel group is the target pattern to detect and the time-series kernel execution graph

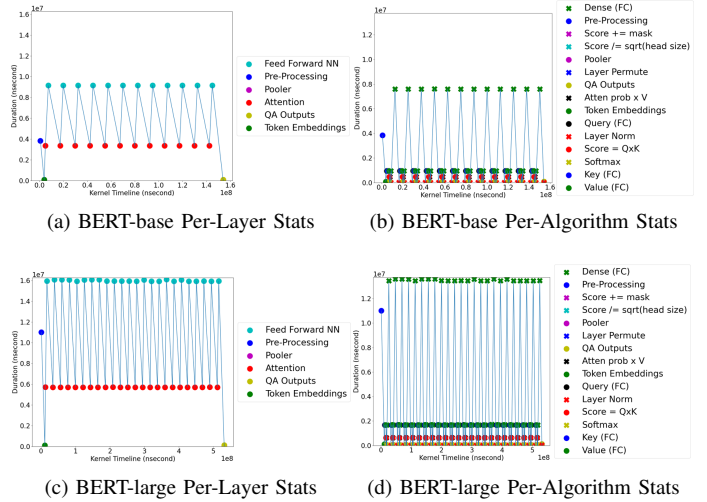


Fig. 14: Execution Times of Layers and Algorithms of BERT PyTorch SQuAD Models Released by NVIDIA

can be considered as an input image. Therefore, we propose to use a CNN model for recovering the victim model architecture. CNN is especially effective for this problem because it can recognize various patterns (divers kernel group shapes) for individual object class (kernel group that corresponds to an encoder). For example, our encoder detection is similar to a vehicle recognition where vehicles with various types and colors can be equally classified to a vehicle.

We explored various architectures and finalized the CNN model with seven hidden layers: conv (in: 3, out: 6, kernel:  $5 \times 5$ ), pool (kernel:  $8 \times 8$ , stride: 8), conv (in: 6, out: 16, kernel:  $5 \times 5$ ), pool (kernel:  $8 \times 8$ , stride: 8), fc (in: 3600, out: 120), fc (in: 120, out: 84), fc (in: 84). The model is trained with time-series kernel execution time graphs. We converted each graph to a gray-scale image where each pixel is colored with either white or black. Each pixel on a x-y tuple as (kernel invocation time, kernel execution time) has black color. We made all graph images uniformly have  $1024 \times 1024$  pixels. The converted graph images were collected while running the inferences of 10 BERT models listed in Table II (except for CNN and GLUE benchmark). The ground truth of each prediction is the number of encoders in the input graph. The number of encoders is the most important parameter that represents a certain BERT model architecture as the widely used BERT-base and BERT-large have static number of encoders. Though BERT-base and BERT-large are the two widely used architectures, we also trained the model by changing the number of encoders gradually such that any victim models that are optimized to use arbitrary number of encoders can be also recovered.

## B. Weight Extraction

1) *Recovering Vendor & Framework*: With a simple CNN model, BERT architectures can be detected. To extract weights, we also need to detect vendor and framework. For this purpose, we propose to develop two more CNN models each predicts vendor and framework of the pre-trained model used by the victim model. This is again similar to vehicle detection but



with a finer-grained prediction that detects types of vehicles separately, such as sedan, truck, suv, and so on. For the training dataset collected for the encoder detection, we re-labeled them to individual vendor and framework. The same CNN architecture worked accurately. We assume that an adversary has a large pool of pre-trained models that are publicly released. With the predicted model architecture, vendor, and framework, the attacker can search the pool of pre-trained models. Once a matching pre-trained model is found, the weight values of the pre-trained model is regarded to be almost similar to the victim fine-tuned model's, as we observed in Section III.

**Model Variants Detection:** Some vendors release several variant models for the same BERT architecture and framework, namely *cased*, *uncased*, *whole word masked* and *sub-word masked*. We found that these variant models show almost alike execution patterns as they follow the same architecture and use similar GPU kernels. For these models, we use special input testing-based recognition by exploiting the dedicated purposes that each model is designed for. For example, a cased model recognizes different meanings when a word is written in upper case and lower case, while an uncased model cannot recognize the differences. Thus, when a context is provided with Apple as a company name and apple as a fruit name used together, the cased model and the uncased model predict differently. Once the variant model is detected, the weight values can be also extracted as described earlier. We tested all four variants of Huggingface BERT-large model and found that the fine-tuned model weights are different with each other with up to 0.25 value distance, while each fine-tuned model and its baseline pre-trained variant model show very high similarity ( $< 0.002$  value distance). Therefore, once vendor, framework, and variant information are detected, almost similar weights can be recovered from the corresponding pre-trained model.

2) *Recovering Actual Weights:* Though our pre-trained model identification recovers all encoder layers' weight values with very small ( $< 0.002$ ) differences, the weight value gap can be further reduced by applying two methods: 1) selective weight checking and 2) heuristic testings. The last classification layer weights can be recovered with the combination of these two methods.

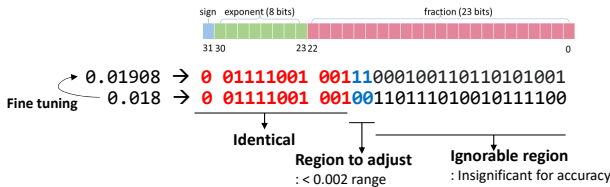


Fig. 15: Selective Value Checking

**Selective Weight Checking with Weight Extraction Pruning:** Selective value checking leverages existing solutions for individual weight value extraction. Some studies used bus probing and some other studies leveraged rowhammer attacks on the victim model (fine-tuned model in our case) [4]. Those studies showed that it is possible to reveal weight values for short data types (e.g., integer values) for CNN models.

However, individual weight value recovery requires hundreds of hammering and bus probing and hence it is not desirable to be used for longer data types such as float16 or float32. But, our weight value similarity can effectively reduce the scope of checking. As pre-trained model and its fine-tuned model has  $< 0.002$  value difference, sign and exponent fields rarely change. From our experiments, we observed that average of around 99% weights keep their sign when fine-tuned. Only the fraction part has differences mostly. Out of them, we found that only one to two bits that correspond to 0.002 range need to be checked. Figure 15 shows an example. When a weight value 0.018 is fine-tuned to 0.01908, the sign and exponent fields are identical. Also, first a few bits of fraction field are identical, as highlighted with red color. Only the two bits in blue color that make the differences between the two values may need checking. The remaining 18 bits in fraction field do not need to be checked because those make differences less than 0.001. From our experiments, we observed that a fine-tuned model provides almost similar accuracy (F1 score is slightly dropped from 87.9078 to 87.8881) when all weights are adjusted to discard values below floating-point fourth digits (e.g., 0.0013 is adjusted to 0.001). Similarly, the number of weights to check can be significantly reduced because the weights that have their absolute value below 0.001 barely have impact for final prediction accuracy and hence can be excluded from checking.

With these observations, we propose *weight extraction pruning*. The pruning is done in two phases on the fine-tuned victim model for the bits that are considered unnecessary for checking, based on the weight value in the pre-trained model found from our vendor/signature detection. First, the weights whose mapping weight's absolute value in the pre-trained model is less than 0.001 are excluded from checking. Second, for the remaining weights, two bits per weight value are only checked which are corresponding to 0.002 value ranges. In the second phase, the bit locations to check may vary depending on the exponent field value and integer part of the weight value. For example, in Figure 15, the most significant 4<sup>th</sup> and 5<sup>th</sup> bits of fraction field are checked because the exponent part value is 121, which means that the value is multiplied by  $2^{121-127} = 2^{-6}$ . This means that the value's implicit integer part is corresponding to 0.015 ( $=2^{-6}$ ) and the fraction part's first 1, which is on the most significant 3<sup>rd</sup> bit is corresponding to 0.0019 ( $=2^{-9}$ ). When adding these two values, the value becomes around 0.0169. As 0.018's potential fine-tuned value range is between 0.016 and 0.02, the following two bits (highlighted with blue color) that each corresponds to 0.00097 ( $=2^{-10}$ ) and 0.00048 ( $=2^{-11}$ ) together make sufficient value range that determines the fine-tuned value. This bit location finding to check can be implemented in a script and the remaining bits can be excluded from checking. With almost similar value baseline acquired from the pre-training model identification, we can make the hammering/probing-based weight-value recovery more feasible for longer data formats. Algorithm 1 is a pseudo code for float32 weights. The algorithm can be revised to support different data formats by changing float32-specific formulas such as *exponent* - 127.

---

**Algorithm 1** Selective Weight Checking with Weight Pruning:  
 Example of float32
 

---

```

target_weight ← Wi in fine-tuned model
base_weight ← Wi in pre-trained model
abs_base_weight ← abs(Wi) in pre-trained model
if base_weight < 0.001 then
  No need to check. clone model's Wi ← base_weight
else
  min ← base_weight − 0.002
  max ← base_weight + 0.002
  k ← most significant non-zero bit location of fraction
  field in abs_base_weight
  int_base ← 2exponent−127 of abs_base_weight
  j ← 2
  while j > 0 do
    fr_base ← 2exponent−127−k of abs_base_weight
    if min ≤ (int_base + fr_base) ≤ max then
      check (hammer) kth bit of target_weight.
      clone model's fraction field kth bit of Wi
      ← fraction field kth bit of target_weight
    end if
    j ← j − 1, k ← k + 1
  end while
end if

```

---

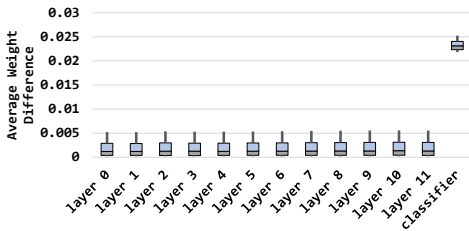


Fig. 16: Average Weight Differences Among 9 BERT-base Models in GLUE benchmark

**Heuristic Testing:** When either row hammering or bus probing can not be used, heuristic testing can be also considered to estimate the actual weight values. Krishna et al. [24] created functionally equivalent clone models through heuristic testing. They picked a random pre-trained BERT model, tested the victim BERT model with a list of inputs that are related to the victim model’s task, and fine-tuned the random model with the outputs of the victim model to clone the victim model. They did not attempt to reveal the actual architecture of the victim model but showed that using the same BERT architecture with the victim model is more effective for cloning. Therefore, an attacker can leverage the heuristic testing over the pre-trained model that is recovered from our model architecture and vendor/signature extractions to estimate the actual weight values. In Section VI-C, we apply the heuristic testing to our attack model and show the benefit of finding the actual architecture of the victim model.

Heuristic testing can be used for reducing the scope of weight value checking for the last classifier layer. The weights of all encoder layers in BERT model are adjusted based off that of the

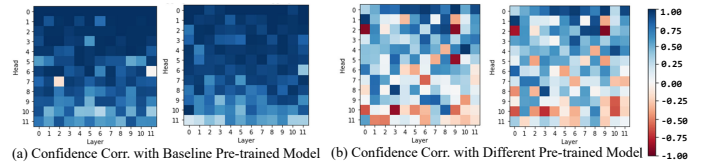


Fig. 17: Pearson Correlation Coefficient of Confidence used for Head Pruning: X-axis is layer and Y-axis is head.

pre-trained model during the fine-tuning. But, the last classifier layer is newly attached to be trained for the fine-tuning task. Thus, the weight value similarity might not be consistently observed. When we checked weight value distance among nine Huggingface GLUE benchmark [25] models that are fine-tuned for different tasks from the same pre-trained model, all the encoder layers had almost zero distance while the last layer showed 10× higher differences than the other layers. Thus, the selective weight pruning might not be directly applicable for the last layer. Instead, we can consider leveraging heuristic testing. With heuristic testing, we can acquire baseline weights of the last layer and then apply selective weight checking to find the actual weight values. This works if the vendor/framework detection is successful, because similar initial weight values (e.g., random seed) are likely to be used for training the last layer.

3) *Supporting Quantization and Pruning:* We explained the weight extraction with an example of float32 data format. However, the victim model might be optimized with quantization and pruning techniques, while pre-trained models are typically released in float32 format for a highly accurate fine-tuning. The popular quantization supported by most of the frameworks are int8, uint8, int16, uint16, int32, bfloat16, and float16. For all floating-point data types, the only differences are the lengths of exponent and fraction fields. For example, compared to float32 data format, float16 uses shorter (5-bit) exponent and (10-bit) fraction fields, while bfloat16 uses the same-length (8-bit) exponent with a shorter (7-bit) fraction field. Therefore, our proposed selective value checking can be directly applied with a slight bit range adjustment. The kernel execution time patterns provide hints for data formats. For example, according to our experiments, kernels using float32 weights have at least 2× longer execution time than float16 weights. The specific data formats used for quantization vary depending on frameworks. Thus, by leveraging the framework information extracted in Section V-B1, the corresponding pre-trained model weight file can be quantized by using the framework supported APIs before extracting actual weights.

The victim model might be optimized for better performance and accuracy. For example, head pruned models are known to have better accuracy and computation efficiency by removing insignificant heads [26], [27]. The head pruning algorithm uses various metrics to identify the removable heads. One of the most popular metrics is *Confidence*, which is calculated by averaging the maximum attention weights. The heads that have lower confidence than a pre-defined threshold are pruned. If the target victim model has some heads pruned, weight extraction will be challenging because weight locations will

not be directly mapped to the unpruned pre-trained model’s. For such case, we believe the attacker can acquire an important hint from the weight value similarity. Because the confidence is calculated based on the weights, if the weights are similar, head confidences are likely to be similar. With the confidence value calculated with pre-trained model’s weight, the attacker can locate the pruned heads. We evaluated the confidence value similarity between a pre-trained model and its two fine-tuned models that are trained for different tasks (semantic equivalence and sentiment analysis) by feeding the same set of input queries as shown in Figure 17(a). Each cell in the matrix is a Pearson correlation coefficient between the confidence of the heads on the same location in a pre-trained model and a fine-tuned model. As the scale bar on the right indicates, darker blue cells mean high correlation while whiter cells mean no correlation. In both fine-tuned models, confidence of all heads are highly correlated with that in the pre-trained model. On the other hand, when we compared the two fine-tuned models and a different pre-trained model, the correlation dropped significantly as plotted in Figure 17(b). From this result, we believe it is challenging but possible to extract head pruning information of a victim model by leveraging the weight value similarity.

## VI. EVALUATION

### A. Methodology

We examined a total of 20 models for evaluation as listed in Table II. 10 pairs (pre-trained and fine-tuned) of BERT/ RoBERTa models are downloaded from four vendors’ repositories to develop a model architecture extraction attack. For a fair comparison, we used whole-word masked and uncased models because some vendors provide only this version models. We intentionally included models from different vendors that use different deep learning frameworks to evaluate the vendor/framework signature extraction accuracy. For these 10 models, we used vendor-provided fine-tuned models rather than designing our own fine-tuned models to avoid any misinterpretation caused by our premature fine-tuning. We also used another nine fine-tuned models that are developed by using the pre-trained model and fine-tuning script of Huggingface GLUE benchmark [25] for verifying the impact of different tasks for the weight value similarity. A ResNet-18 model is also fine-tuned based on the pre-trained model downloaded from PyTorch vision repository [28] to examine the scalability of our approach to non-Transformer model. We tested these models on a laptop that has NVIDIA GeForce GTX 1660Ti (Turing) GPU with CUDA v11.5 as well as a server that has NVIDIA V100 (Volta) GPU with CUDA v11.1. We used Python v3.8, PyTorch v1.11.0, and TensorFlow v2.8.0 for evaluations.

### B. Model Architecture Extraction Accuracy

We trained the CNN-based architecture, vendor, and framework extraction attack models with 5-fold cross validation on a total of 680 profiled data. 136 data were used for testing. Thanks to the notable execution patterns, vendor, framework, and encoder count were predicted with 96.30%, 99.85%, and 90.07% accuracy, respectively.

TABLE II: 20 Tested Models: The models are trained for the tasks (with datasets) in *Pre-trained* and *Fine-tuned* columns.

Model	Vendor	Framework	Pre-trained	Fine-tuned
BERT-Base	NVIDIA [15]	PyTorch	MLM/NSP	SQuAD
	NVIDIA [16]	TensorFlow		
	Huggingface [13]	PyTorch	MLM/NSP	SQuAD
	Huggingface [29]	TensorFlow		
BERT-Base	Huggingface GLUE benchmark [25]	PyTorch	MLM/NSP	CoLA SST-2 MRPC STS-B QQP MNLI QNLI RTE WNLI
	NVIDIA [15]	PyTorch	MLM/NSP	SQuAD SST-2
	NVIDIA [16]	TensorFlow		SQuAD
	Huggingface [13] Huggingface [29]	PyTorch TensorFlow	MLM/NSP	SQuAD
RoBERTa-Large	Meta [14]	PyTorch	MLM	MNLI
ResNet-18	Meta [28]	PyTorch	ImageNet’12	Hymenoptera

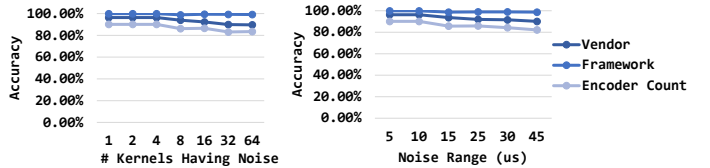


Fig. 18: Extraction Accuracy with Kernel Execution Time Measurement Noise: (left) impact of kernel count having noise (right) impact of noise lengths

**Noise Sensitivity :** We evaluated the prediction accuracy by adding noise to the kernel execution time measurements. We evaluated noise sensitivity in two ways: 1) varying the scope of kernels impacted by noise 2) varying significance of noise for individual kernels. Based on the typical kernel duration, we set the noise in the first test to 20 us. We randomly selected  $N$  kernels from one of the input images used for the CNN model inference and adjusted their execution time to *original execution time*  $\pm 20us$ , while varying  $N$  from 1 to 64. For the second test, we selected 16 kernels from one of the validation images and changed their execution times to *original execution time*  $\pm Kus$ , where  $K$  is varied from 5 to 45 us. Then, the adjusted time-series kernel execution images are fed to all CNN models for vendor, framework, and architecture prediction. Figure 18 shows the accuracy results. As plotted in the figure, accuracy was dropped very slowly for both cases. This is because CNN architecture is inherently error-tolerant [30].

### C. Model Cloning Accuracy

We evaluated the effectiveness of heuristic testing. We used the same method as used by Krishna et al. [24], except for that the adversary can extract the victim model architecture and hence use the correct pre-trained model for heuristic testing. To compare with Krishna’s approach, we also selected random pre-trained models for attack baseline models that either uses different BERT architecture or uses the correct BERT architecture but created by different vendor. Then, we fed 87599 inputs to the victim model and collected the corresponding outputs. The attack baseline models were fine-tuned with 87589

input and output pairs collected from the victim model. Note that the output here is not the dataset’s ground truth; it is victim model’s outputs because the goal of this attack is to create a clone of the victim model. Two epochs were used with  $3e-05$  as learning rate. Then, we tested the clone models with the remaining 10 inputs and evaluated the accuracy and prediction similarities with the victim model. The model that used correct pre-trained model showed 100% identical outputs with the victim model while the models that used random pre-trained model derived 90% similarity with the victim model. The clone models that used the same BERT architecture with the victim model derived similar F1 scores with the victim model (87.9078, 88.3654, and 88.026), while the clone model that used a larger (BERT-large) pre-trained model showed even better F1 score, which is 89.97366. This is because BERT-large models can extract more complex relations better than BERT-base models due to larger and more encoders. However, as the attack goal is to make a clone of the victim model, not creating an outperforming model, our recovered pre-trained model showed a better capability to copy the victim model than randomly selected models.

#### D. Weight Extraction Efficiency



Fig. 19: Reduced Weight Value Checking w/o Errors

To understand the efficiency of weight extraction pruning, we examined weight values of a randomly selected pre-trained model and its fine-tuned model and measured the total number of bits that need to be checked. As proposed, we excluded values that are smaller than 0.001 from checking. For the remaining weights, we excluded all bits except for 2 bits in fraction field from checking. As attackers will have access to the pre-trained model only, we simulated their attempts by excluding weights based on the values in the pre-trained model. We verified the pruning accuracy by checking the fine-tuned weight values. If the value change is larger than 0.002 or the sign bit is changed, we considered that the pruning leads to incorrect extraction. Figure 19 shows the reduced checking breakdown. The *Weights* bar chart shows the total number of weights correctly pruned. The *Bits* bar chart shows the total number of bits (when considering 32-bit single precision weights) correctly excluded from checking. From the weight checking pruning, we were able to exclude 90% weights and 85% bits of weights from checking.

#### E. Applicability to non-Transformer Models

We believe the weight value similarity is not a unique characteristics of Transformer models. All models that use transfer learning may have the same issue. To verify our intuition, we measured per-layer weight difference of a popular

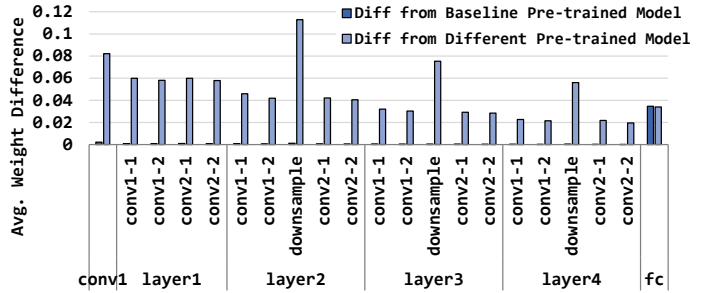


Fig. 20: Weight Similarity in a CNN Model (ResNet-18)

CNN model, ResNet-18, between a fine-tuned model and its baseline pre-trained model as plotted in Figure 20. We downloaded a pre-trained model from the PyTorch Vision repository [28] and fine-tuned it with Hymenoptera database. For a comparison, we trained another ResNet-18 model with the same Hymenoptera database from scratch (without using transfer learning) and compared the weight values with the aforementioned fine-tuned model. The darker blue bar chart in the figure is the weight difference between the fine-tuned model and its baseline pre-trained model. The lighter bar chart is the compared result with a model that is trained from scratch. As clearly noticed, the fine-tuned model has almost zero ( $\approx 0.002$ ) weight difference from the baseline pre-trained model in almost all layer, while it shows at least  $10\times$  higher difference from a different model even when they are trained with the same database. We believe this weight similarity is sourced from various parameters used in the initial training such as random seed values. Therefore, we believe this phenomenon will be observed from any models that use transfer learning and hence our weight value similarity-based model extraction attack is applicable for wider range of models.

## VII. POTENTIAL COUNTER MEASURES

For model extraction attacks, we believe that the root cause is consistent execution patterns. To break the execution consistency, we showed that some vendor/framework-specific optimizations make notable noises. However, if the noise also has some patterns, as we found from TensorFlow XLA examples, it is only a matter of time that attackers understand the pattern. Therefore, the same optimizations should not be used all the time. Employing bogus kernels or thread blocks have been studied to obfuscate GPU kernel executions [31]. However, bogus kernels incur significant performance overhead. To catch both performance and security with one solution, we can consider randomizing the selections of GPU kernels/libraries and usages of various optimizations. Though there are only handful of GPU deep learning libraries (e.g., cuDNN, cuBLAS), an algorithm (e.g., tensor calculation) can be executed with various combinations of library functions. If the combination selection is randomly determined at run time, it would be challenging to extract computation patterns. For example, if one long kernel execution is partitioned into many short kernels, the execution pattern will look very different. Regarding weight value similarity between pre-trained and fine-tuned models,

one easiest way is to apply different quantization for fine-tuned models. However, due to limited quantization options as discussed in Section V-B3, it would be eventually understood by the attackers. Instead, we can consider encoding the fine-tuned weights with homomorphic encryption [32], [33] that can be directly computed without decryption. However, the area and performance of homomorphic encryption would be another hurdle to resolve.

## VIII. RELATED WORK

### A. Model Extraction Attack

Several studies demonstrated various model extraction attacks [1], [4], [34], [35], [36], [37], [38]. The target models range from basic machine-learning (ML) models like linear regression and support vector machine to most recent neural network models. Tramèr et al. [34] demonstrated an ML model extraction through iterative request transfer to Machine-Learning-as-a-Service servers. Hu et al. and Naghibijouybari et al. [1], [2] proposed a framework to extract a black-box CNN model architecture by modeling the mapping between GPU architectural hints and model architecture as a ML recognition problem. Zhu et al. [35] proposed a technique to clone CNN model weights by monitoring and analyzing unencrypted PCIe bus traffic. Yan et al. [3] introduced a side-channel attack for model extraction based on cache behaviour. Roberts et al. [37] demonstrated that attackers can extract victim model weights by injecting random noise inputs to softmax layers. They assume that the attacker is aware of the victim model architecture and has access to softmax layer. Rakin et al. [4] leveraged RowHammer [39] attack to recover weight values of victim models. For 8-bit weights, they were able to recover almost perfect value with over 4000 rounds of hammerings. **These earlier studies mostly targeted CNN models, while we propose a new model extraction attack for Transformer models by leveraging security vulnerabilities of transfer learning.**

### B. Attack on Transformer Models

As Transformer models become more popular due to their state-of-the-art performance in various ML domains, there have been several studies that tackled security concerns about Transformer models. Some studies [24], [40], [41] created clone models of a victim BERT model through heuristic testings. By feeding a few random inputs and collecting the predictions of a victim BERT model through online BERT API query services, they were able to train a model that predicts almost similarly (or even better) with the victim model. As their attack goal was not revealing the model architecture, they used a randomly selected BERT pre-trained model. Their experimental results show that the clone model that is built with the same model architecture with the victim model produces more similar predictions. Some other studies revealed vulnerabilities of algorithms used by Transformer models [42], [43], [44], [45]. They leveraged token-level or sentence-level adversarial samples to attack the victim model in either training phase or inference phase. **These prior works either focus on the theoretical/empirical**

**analysis on ML characteristics of the Transformer models or reproduce a functionally similar model as the victim online serving model. We provide a comprehensive analysis on the security problems issued by the publicly accessible pre-trained models.**

## IX. CONCLUSION

This paper raises a new security concern for transfer-learning models. We show that vendor and framework signature can be leveraged to locate the pre-trained model that the victim model is fine-tuned with. The identified pre-trained model becomes a good source of revealing almost similar weight values in the entire model level. We design a CNN model for the automated model extraction and propose methods to recover actual weights.

## REFERENCES

- [1] X. Hu, L. Liang, S. Li, L. Deng, P. Zuo, Y. Ji, X. Xie, Y. Ding, C. Liu, T. Sherwood, and Y. Xie, "DeepSniffer: A DNN Model Extraction Framework Based on Learning Architectural Hints," in *Conference on Architectural Support for Programming Languages and Operating Systems*, 2020.
- [2] H. Naghibijouybari, A. Neupane, Z. Qian, and N. Abu-Ghazaleh, "Rendered Insecure: GPU Side Channel Attacks are Practical," in *ACM Conference on Computer and Communications Security*, 2018.
- [3] M. Yan, C. W. Fletcher, and J. Torrellas, "Cache Telepathy: Leveraging Shared Resource Attacks to Learn DNN Architectures," in *USENIX Security Symposium*, 2020.
- [4] A. S. Rakin, M. H. I. Chowdhury, F. Yao, and D. Fan, "DeepSteal: Advanced Model Extractions Leveraging Efficient Weight Stealing in Memories," *IEEE Symposium on Security and Privacy*, 2022.
- [5] J. Devlin, M.-W. Chang, K. Lee, and K. Toutanova, "BERT: Pre-training of deep bidirectional transformers for language understanding," *arXiv:1810.04805*, 2018.
- [6] A. Radford, J. Wu, R. Child, D. Luan, D. Amodei, and I. Sutskever, "Language Models are Unsupervised Multitask Learners," *OpenAI*, vol. 1, no. 8, p. 9, 2019.
- [7] T. Brown, B. Mann, N. Ryder, M. Subbiah, J. D. Kaplan, P. Dhariwal, A. Neelakantan, P. Shyam, G. Sastry, A. Askell, S. Agarwal, A. Herbert-Voss, G. Krueger, T. Henighan, R. Child, A. Ramesh, D. Ziegler, J. Wu, C. Winter, C. Hesse, M. Chen, E. Sigler, M. Litwin, S. Gray, B. Chess, J. Clark, C. Berner, S. McCandlish, A. Radford, I. Sutskever, and D. Amodei, "Language Models are Few-Shot Learners," *Advances in Neural Information Processing Systems*, vol. 33, pp. 1877–1901, 2020.
- [8] Huggingface BERT-base Pre-trained Model. [Online]. Available: <https://huggingface.co/bert-base-uncased>
- [9] Huggingface Distilled GPT-2 Pre-trained Model. [Online]. Available: <https://huggingface.co/distilgpt2>
- [10] A. Vaswani, N. Shazeer, N. Parmar, J. Uszkoreit, L. Jones, A. N. Gomez, L. Kaiser, and I. Polosukhin, "Attention Is All You Need," *arXiv:1706.03762*, 2017.
- [11] Y. Liu, M. Ott, N. Goyal, J. Du, M. Joshi, D. Chen, O. Levy, M. Lewis, L. Zettlemoyer, and V. Stoyanov, "RoBERTa: A Robustly Optimized BERT Pretraining Approach," *arXiv:1907.11692*, 2019.
- [12] Z. Lan, M. Chen, S. Goodman, K. Gimpel, P. Sharma, and R. Soricut, "ALBERT: A Lite BERT for Self-supervised Learning of Language Representations," in *International Conference on Learning Representations*, 2020.
- [13] Huggingface BERT PyTorch. [Online]. Available: [https://huggingface.co/docs/transformers/v4.17.0/en/model\\_doc/bert](https://huggingface.co/docs/transformers/v4.17.0/en/model_doc/bert)
- [14] Meta RoBERTa PyTorch. [Online]. Available: <https://github.com/pytorch/fairseq/tree/main/examples/roberta>
- [15] NVIDIA BERT PyTorch. [Online]. Available: <https://github.com/NVIDIA/DeepLearningExamples/tree/master/PyTorch/LanguageModeling/BERT>
- [16] NVIDIA BERT TensorFlow. [Online]. Available: <https://github.com/NVIDIA/DeepLearningExamples/tree/master/TensorFlow2/LanguageModeling/BERT>

- [17] DeepSniffer ResNet Models. [Online]. Available: <https://github.com/xinghu7788/DeepSniffer/>
- [18] NVIDIA ResNet v1.5 for PyTorch. [Online]. Available: [https://catalog.ngc.nvidia.com/orgs/nvidia/resources/resnet\\_50\\_v1\\_5\\_for\\_pytorch](https://catalog.ngc.nvidia.com/orgs/nvidia/resources/resnet_50_v1_5_for_pytorch)
- [19] TensorFlow ResNet Models. [Online]. Available: [https://tfhub.dev/google/imagenet/resnet\\_v2\\_50/classification/5](https://tfhub.dev/google/imagenet/resnet_v2_50/classification/5)
- [20] MXNet ResNet Models. [Online]. Available: [https://github.com/apache/incubator-mxnet/blob/master/python/mxnet/gluon/model\\_zoo/vision/resnet.py](https://github.com/apache/incubator-mxnet/blob/master/python/mxnet/gluon/model_zoo/vision/resnet.py)
- [21] R. Callan, A. Zajić, and M. Prvulovic, "A Practical Methodology for Measuring the Side-Channel Signal Available to the Attacker for Instruction-Level Events," in *IEEE/ACM International Symposium on Microarchitecture*, 2014.
- [22] C. Luo, Y. Fei, P. Luo, S. Mukherjee, and D. Kaeli, "Side-Channel Power Analysis of a GPU AES Implementation," in *IEEE International Conference on Computer Design*, 2015.
- [23] XLA: Optimizing Compiler for Machine Learning. [Online]. Available: <https://www.tensorflow.org/xla>
- [24] K. Krishna, G. S. Tomar, A. P. Parikh, N. Papernot, and M. Iyyer, "Thieves on Sesame Street! Model Extraction of BERT-based APIs," in *International Conference on Learning Representations*, 2020.
- [25] Huggingface General Language Understanding Evaluation (GLUE) Benchmark. [Online]. Available: <https://github.com/huggingface/transformers/tree/main/examples/pytorch/text-classification#glue-tasks>
- [26] E. Voita, D. Talbot, F. Moiseev, R. Sennrich, and I. Titov, "Analyzing Multi-Head Self-Attention: Specialized Heads Do the Heavy Lifting, the Rest Can Be Pruned," in *Annual Meeting of the Association for Computational Linguistics*, 2019.
- [27] E. Voita, R. Sennrich, and I. Titov, "Analyzing the Source and Target Contributions to Predictions in Neural Machine Translation," in *Annual Meeting of the Association for Computational Linguistics*, 2021.
- [28] Pytorch Hub: Repository of Pre-trained models. [Online]. Available: <https://pytorch.org/docs/stable/hub.html>
- [29] Huggingface BERT TensorFlow. [Online]. Available: [https://huggingface.co/docs/transformers/model\\_doc/bert#transformers.TFBertForQuestionAnswering](https://huggingface.co/docs/transformers/model_doc/bert#transformers.TFBertForQuestionAnswering)
- [30] G. Li, S. K. S. Hari, M. Sullivan, T. Tsai, K. Pattabiraman, J. Emer, and S. W. Keckler, "Understanding Error Propagation in Deep Learning Neural Network (DNN) Accelerators and Applications," in *Proceedings of the International Conference for High Performance Computing, Networking, Storage and Analysis*, 2017.
- [31] G. Kadam, D. Zhang, and A. Jog, "BCoal: Bucketing-Based Memory
- [40] Q. Xu, X. He, L. Lyu, L. Qu, and G. Haffari, "Beyond Model Extraction: Imitation Attack for Black-Box NLP APIs," *abs/2108.13873*, 2021.
- Coalescing for Efficient and Secure GPUs," in *International Symposium on High Performance Computer Architecture*, 2020.
- [32] A. Feldmann, N. Samardžić, A. Krastev, S. Devadas, R. Dreslinski, K. Eldefrawy, N. Genise, C. Peikert, and D. Sanchez, "F1: A Fast and Programmable Accelerator for Fully Homomorphic Encryption," in *IEEE/ACM International Symposium on Microarchitecture*, 2021.
- [33] S. Kim, J. Kim, M. J. Kim, W. Jung, M. Rhu, J. Kim, and J. H. Ahn, "BTS: An Accelerator for Bootstrappable Fully Homomorphic Encryption," in *International Symposium on Computer Architecture*, 2022.
- [34] F. Tramèr, F. Zhang, A. Juels, M. K. Reiter, and T. Ristenpart, "Stealing Machine Learning Models via Prediction APIs," in *USENIX Security Symposium*, 2016.
- [35] Y. Zhu, Y. Cheng, H. Zhou, and Y. Lu, "Hermes Attack: Steal DNN Models with Lossless Inference Accuracy," in *USENIX Security Symposium*, 2021.
- [36] M. Yan, C. W. Fletcher, and J. Torrellas, "Cache Telepathy: Leveraging Shared Resource Attacks to Learn DNN Architectures," in *USENIX Security Symposium*, 2020.
- [37] N. Roberts, V. U. Prabhu, and M. McAteer, "Model Weight Theft With Just Noise Inputs: The Curious Case of the Petulant Attacker," *abs/1912.08987*, 2019.
- [38] Z. Yue, Z. He, H. Zeng, and J. McAuley, "Black-Box Attacks on Sequential Recommenders via Data-Free Model Extraction," in *ACM Conference on Recommender Systems*, 2021.
- [39] Y. Kim, R. Daly, J. Kim, C. Fallin, J. H. Lee, D. Lee, C. Wilkerson, K. Lai, and O. Mutlu, "Flipping Bits in Memory Without Accessing Them: An experimental study of DRAM disturbance errors," *ACM SIGARCH Computer Architecture News*, vol. 42, no. 3, pp. 361–372, 2014.
- [41] L. Lyu, X. He, F. Wu, and L. Sun, "Killing Two Birds with One Stone: Stealing Model and Inferring Attribute from BERT-based APIs," *abs/2105.10909*, 2021.
- [42] K. Mahmood, R. Mahmood, and M. Van Dijk, "On the Robustness of Vision Transformers to Adversarial Examples," in *IEEE/CVF International Conference on Computer Vision*, 2021.
- [43] Z. Wei, J. Chen, M. Goldblum, Z. Wu, T. Goldstein, and Y.-G. Jiang, "Towards Transferable Adversarial Attacks on Vision Transformers," *arXiv:2109.04176*, 2021.
- [44] C. Guo, A. Sablayrolles, H. Jégou, and D. Kiela, "Gradient-based Adversarial Attacks against Text Transformers," in *Conference on Empirical Methods in Natural Language Processing*, 2021.
- [45] A. Joshi, G. Jagatap, and C. Hegde, "Adversarial Token Attacks on Vision Transformers," *arXiv:2110.04337*, 2021.